Journal of the European Ceramic Society 19 (1999) 2503–2509

PII: S0955-2219(99)00100-4
0955-2219/99/$ - see front matter

Residual Stresses in High-temperature Ceramic Eutectics

Elizabeth C. Dickey, [a]* Colleen S. Frazer, [a] Thomas R. Watkins [b] and Camden R. Hubbard [b]

[a]Department of Chemical and Materials Engineering, University of Kentucky, Lexington, KY 40506-0046, USA
[b]High Temperature Materials Laboratory, Metals and Ceramics Division, Oak Ridge National Laboratory, Oak Ridge, TN 37831, USA

Abstract

This paper explores residual thermal stresses in directionally solidified ceramic eutectics, a class of materials that has much promise for high-temperature structural applications. Residual strain tensors of both phases in a eutectic composite are measured by single crystal X-ray diffraction techniques. In the analysis the material is treated as fully anisotropic and the strain tensors, subsequently converted to stress tensors, are measured. Results are presented for two oxide eutectics, NiO–cubic ZrO_2 and YAG–Al_2O_3, the former having a large thermal expansion mismatch between the two phases and the latter having similar thermal expansion properties. It is discovered that large residual stresses (of the order of 1 GPa) can be present at room temperature in as-processed eutectic materials unless the thermal expansion behaviors of the constituent materials are very similar. Ultimately these measurements not only elucidate the stress state but, when compared to theory, give information about the degree of interfacial constraint between the two phases. © *1999 Elsevier Science Ltd. All rights reserved.*

Keywords: residual stresses, ZrO_2–NiO, Al_2O_3–YAG, eutectics, X-ray methods.

1 Introduction

Residual stresses are of great concern in high-temperature ceramic composites, especially those subject to thermal cycling, because residual stresses ultimately affect the mechanical behavior of the material.[1,2] The primary residual stresses found in composite materials originate from the inevitable thermal expansion mismatch between the two or more constituent phases. Even in monolithic ceramics, thermal stresses can arise between the various grains in the specimen as a consequence of thermal expansion anisotropy. The magnitudes of the thermal residual stresses depend upon several factors, namely (1) the differences in the thermal expansion response, (2) the degree of microstructural and/or interfacial constraint, (3) the material compliances and (4) the plastic responses of the two materials.

In general, in the absence of a compatibility constraint each phase will deform independently as a function of temperature according to the tensor equation:

$$\varepsilon_{ij} = \alpha_{ij}(T - T_o)$$

in which ε_{ij} is the strain tensor and α_{ij} is the tensor containing the coefficients of thermal expansion.[3] As illustrated in Fig. 1 for the case of a lamellar composite, the resultant strains must be the same for both crystals along the direction of the constraint. The resulting compatibility stresses will be at a maximum if no stress-limiting processes such as slip transpire. If the stresses are partially mitigated by plastic deformation, then the compatibility stresses will be reduced in proportion to the plastic deformation that occurs.

One class of high-temperature composites, directionally solidified eutectics (DSEs), based on psuedo-binary oxide eutectics are being sought as high temperature structural or reinforcing materials because many maintain high strengths and creep resistances at elevated temperatures.[4–7] Oxide eutectic temperatures are usually higher than 1700°C, so during the solidification processing, enormous residual stresses can accumulate in the material if there are appreciable differences in the thermal expansions between the two phases. A complicating factor in modeling thermal residual stresses for this class of composites is that the DSEs are very anisotropic with respect to microstructure and crystallography. To a large extent,

*To whom correspondence should be addressed. Fax: +1-606-323-1929; e-mail: ecdickey@engr.uky.edu

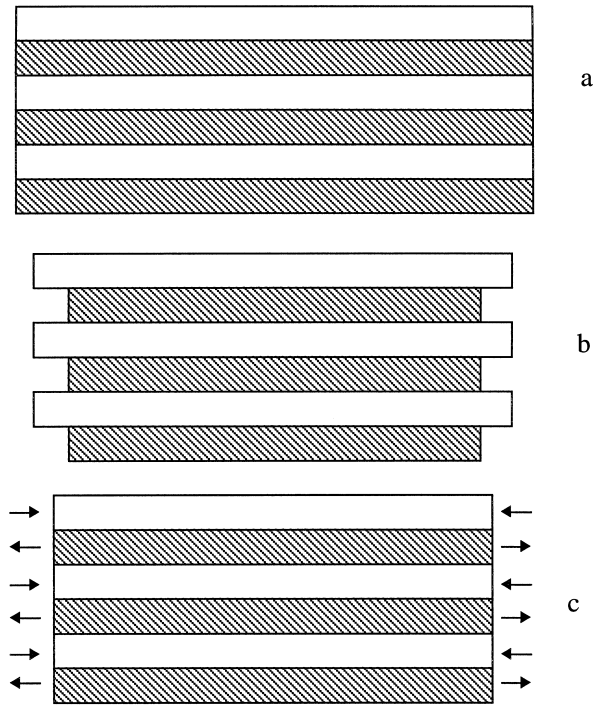

Fig. 1. Origins of residual stresses in laminate composites: (a) laminate at eutectic temperature, stress free; (b) laminate at room temperature with no compatibility constraint; (c) laminate at room temperature with interfacial constraint (the arrows represent residual stresses).

the microstructure of DSEs is determined by the volume fraction of the minor phase. With the criterion of minimum interfacial energy per unit volume, fibrous microstructures are energetically favorable when the volume fraction of the minor phase is less than 0·28, while higher volume fractions lead to lamellar microstructures.[8] Some eutectic systems do not, however, obey this general rule and have more irregular microstructures. Most DSE systems, even those with irregular microstructures, have very well defined crystallographic orientation relationships between the two phases.[9–12] This results in the material being single-crystal-like and necessitates that material anisotropy be taken into consideration when modeling or measuring the thermal residual stresses. Most continuum models which are used to predict composite residual stresses, however, assume material isotropy; this is not a safe assumption for highly oriented composites even when the constituent phases are cubic.

Another complicating factor in predicting residual stresses is that any continuum model must make some implicit assumptions about the degree of interfacial constraint between the two phases. Because it not known *a priori* if stress-limiting processes transpire, or over what temperature ranges they occur, it is difficult to predict the degree of interfacial constraint and it is thus not possible to calculate the magnitude of the resultant stresses with a high degree of confidence. We can, however, experimentally measure the residual strains in the composites using X-ray diffraction techniques and then calculate the residual stress tensors. The residual stress tensor can, in turn, provide information about the degree of interfacial or microstructural constraint.

2 Methods for measuring residual stresses in single crystal composites

Because directionally solidified eutectics are nearly single crystalline, conventional residual stress measurements techniques[13] suited for polycrystalline materials cannot be utilized. The premise behind measuring residual stresses in crystallographically random materials is that residual stresses cause a change in the interplanar spacings in the material along different directions in the sample. So, if interplanar spacings are measured as a function of sample orientation, the residual strain tensor can be extracted and the stress tensor subsequently calculated. For monolithic materials, it is often not necessary to know the unstressed lattice parameter since it is assumed that the normal stresses at the sample surface must converge to zero to satisfy static equilibrium.[13] Furthermore, the analysis is simplified by the random nature of the material which allows diffraction elastic constants to be used in converting the strain tensor to a stress tensor.

In single crystal composites, such as directionally solidified eutectics, measuring residual stresses is much more complicated, and the full thermal and elastic anisotropies of the materials must be taken into account. Moreover, since the average microstresses for each phase are measured, the residual stresses normal to the surface do not necessarily converge to zero; only the integral of the stresses over both phases must sum to zero. This requires independent measurements of the unstressed lattice parameters to be made for each phase. The premise behind measuring residual stresses in single crystals is the same as that for polycrystalline materials in that interplanar spacings are measured along different directions within the sample. The difference is that particular directions in the sample necessarily correspond to crystallographically distinct directions as well.

Because DSEs are usually single or coarse-grained, single grains can be isolated and single-crystal X-ray diffraction techniques can be utilized to measure average microstrains, similar to analyses of other coarse-grained materials.[14–17] Experimentally, strain measurements can be made on a four-circle goniometer diffractometer, so that the crystal can be rotated in any direction (see Ref.18 for a detailed explanation of the experimental

setup). By rotating the goniometer by a combination of χ and ϕ degrees, a particular diffraction vector corresponding to (hkl) is brought into the diffraction plane. Then a Θ–2Θ scan is made across the reflection to measure its d-spacing. To reduce measurement errors, reflections belonging to the same family of planes are measured when possible.[19] Figure 2 shows the reflections employed for strain measurements of $Y_3Al_5O_{12}$ (YAG) in a YAG–Al_2O_3 DSE, to be discussed below. Because YAG is cubic, the d-spacing of each of these set of planes will be identical in the unstressed material. In the presence of residual stresses, however, variations in the d-spacings will be observed.

From at least six d-spacings measured from different crystallographic planes ($d_{hkl}^{\phi\chi}$) and the stress-free lattice parameter (d_o), the strain tensor is calculated according to eqns. (1) and (2) in which $e_{hkl}^{\phi\chi}$ is the measured strain for reflection (hkl) located at ϕ and χ, a_i is the direction cosine between the (hkl) reflection and axis i, and ε'_{ij} is the strain tensor referred to the sample coordinate system.

$$e_{\mathrm{hkl}}^{\phi\chi} = \frac{\mathrm{d}_{\mathrm{hkl}}^{\phi\chi} - d_o}{\mathrm{d}_o} \tag{1}$$

$$e_{\mathrm{hkl}}^{\phi\chi} = a_i a_j \varepsilon'_{ij} \tag{2}$$

Although only six measurements are required to solve for the six components of the symmetric strain tensor, $\boldsymbol{\varepsilon}'_{\mathbf{ij}}$, more than six measurements improve the accuracy of the solution. The generalized least-squares method is employed for overdetermined systems to calculate the strain tensor, $\boldsymbol{\varepsilon}'_{\mathbf{ij}}$, which best fits the experimental data.[20] The strain tensor, $\boldsymbol{\sigma}'_{\mathbf{ij}}$, is subsequently calculated according to eqn (3):

$$\boldsymbol{\sigma}'_{\mathbf{ij}} = \mathbf{C}'_{\mathbf{ijkl}} \boldsymbol{\varepsilon}'_{\mathbf{kl}} \tag{3}$$

in which $\mathbf{C}'_{\mathbf{ijkl}}$ is the single-crystal stiffness tensor referred to the bicrystal coordinate system.[3]

The experimental procedure and data analysis outlined above were employed to measure the residual strain and stress tensors of two DSE composites. A four-circle goniometer powder x-ray diffractometer with a Cu rotating anode source was employed for all experiments. The first DSE system examined, NiO–cubic ZrO_2, is an example of a lamellar composite in which there is an appreciable difference between the two thermal expansion behaviors of the two phases. The second system is YAG-Al_2O_3 in which the thermal expansions are fairly similar but which has a more complex, irregular microstructure.

3 Case study I: NiO–cubic ZrO_2

In the NiO–ZrO_2 (9 mol% Y_2O_3) system, NiO has a volume fraction of 0·44 and the DSE therefore maintains a lamellar microstructure.[21] The predominant crystallographic relationship between the two phases, as depicted in Fig. 3, is:

$$[\bar{1}10]_{\mathrm{NiO}} // [010]_{\mathrm{ZrO_2}} // \text{growth direction}$$

$$(111)_{\mathrm{NiO}} // (100)_{\mathrm{ZrO_2}} // \text{interface plane}$$

Because the two phases are cubic, the thermal expansions are isotropic. Elastically, however, the two materials are anisotropic. Table 1 presents the elastic constants for both materials and the Zener (Z) ratio, a measure of the elastic anisotropy for

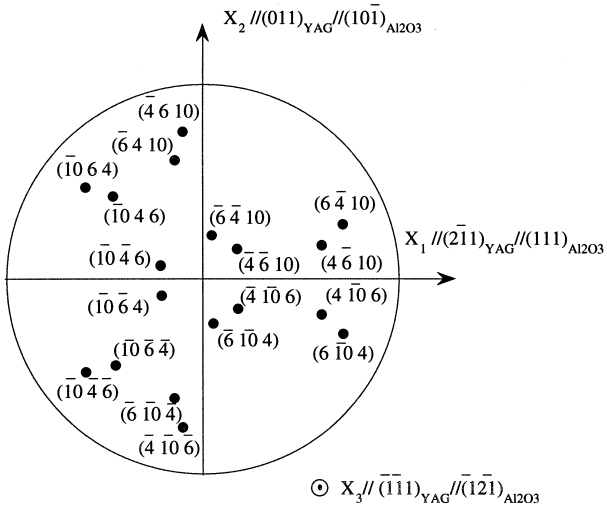

Fig. 2. Stereographic projection showing the 18 {10 6 4} reflections used to measure the residual strain tensor of YAG in a YAG–Al_2O_3 DSE.

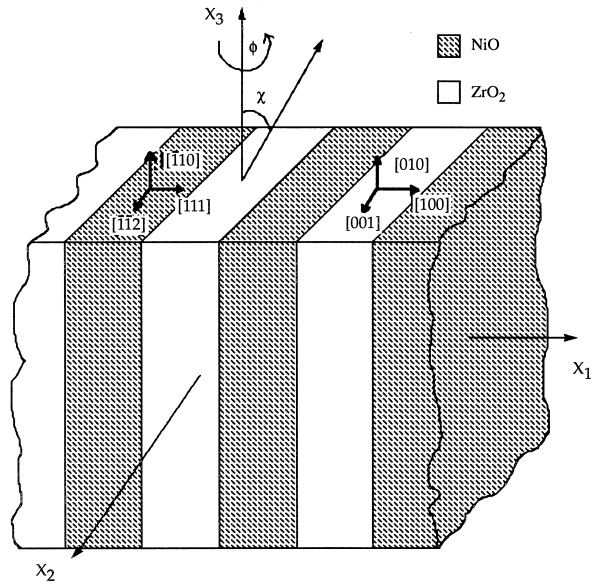

Fig. 3. Schematic of NiO–cubic ZrO_2 grain defining the crystallographic orientation relationship between the two phases and the sample reference frame, defined by x_1, x_2 and x_3.

Table 1. Compilation of single-crystal properties

Property		*NiO*	*ZrO_2*	*YAG*	*Al_2O_3*
Crystal class		Cubic	Cubic	Cubic	Trigonal
CTE [$\times 10^6$ (°C)]		16·5[23]	12·9[23]	8·9[24]	a:9·1[23] c:9·9
Elastic constants:	C_{11}	270 GPa[25]	380 GPa[26]	334 GPa[27]	495 Gpa[27]
	C_{12}	125 GPa	130 GPa	112 GPa	160 GPa
	C_{44}	105 Gpa	59 Gpa	115 Gpa	146 GPa
	C_{33}	—	—	—	497 GPa
	C_{13}	—	—	—	115 GPa
	C_{14}	—	—	—	−23 GPa
Zener ratio $2C_{44}/(C_{11}-C_{12})$		1·45	0·47	1·04	—

cubic crystals. For isotropic materials $Z=1$. The Zener ratio for NiO is 1·45 and for ZrO_2 is 0·47, indicating that both are significantly anisotropic.

Using the experimental methods described above, the residual stress tensors were measured for each phase. The results are presented below along with estimated errors corresponding to one standard deviation:[18]

NiO:

$$\sigma = \begin{bmatrix} -214 & -30 & 9 \\ -30 & 912 & 41 \\ 9 & 41 & 880 \end{bmatrix} \pm \begin{bmatrix} 24 & 7 & 6 \\ 6 & 22 & 10 \\ 6 & 10 & 19 \end{bmatrix} \text{(MPa)}$$

ZrO_2

$$\sigma = \begin{bmatrix} -155 & -3 & -37 \\ -3 & -1099 & -82 \\ -37 & -82 & -1121 \end{bmatrix} \pm \begin{bmatrix} 101 & 8 & 8 \\ 8 & 104 & 20 \\ 8 & 20 & 110 \end{bmatrix} \text{(MPa)}$$

Here x_{11} is normal to the lamellae and x_{22} and x_{33} are within the plane of the lamellae, with x_{33} parallel to the growth direction (see Fig. 3). The most significant stresses are found within the plane of the lamellae (σ_{22} and σ_{33}) and are tensile in NiO and compressive in ZrO_2. The signs of the stresses are in agreement with NiO having a higher coefficient of thermal expansion (see Table 1). Taking into account the volume fractions of the two phases, the sum of these forces balance to zero within the experimental error, satisfying static equilibrium.[18] The magnitude of the stresses indicate that very little stress-mitigating processes such as creep transpire as the eutectic cools from its solidification temperature. This is in agreement with transmission electron microscopy (TEM) data that shows no evidence for interface microcracks or dislocations.[22]

4 Case study II: YAG–Al_2O_3

One of the reasons that YAG–Al_2O_3 composites are good candidates for high-temperature structural materials is that their thermal expansion properties are very similar (see Table 1). Because there is a eutectic between the two phases, it is possible to produce *in situ* composites via directional solidification.[6,28] The volume fraction of YAG is 45%, so a lamellar microstructure would be predicted by simple theories.[8] The microstructure, however, is not lamellar and has a complex geometry (see Fig. 4), so the stress state will necessarily be more complicated than that of the ideal lamellar or fibrous microstructures. The other complicating factor in modeling residual stresses in this system is that alumina is not cubic so both its

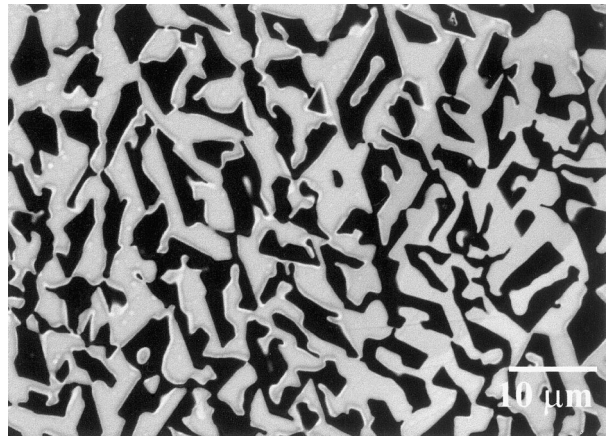

Fig. 4. SEM backscattered electron image of YAG–Al_2O_3 DSE showing the irregular Chinese script microstructure.

thermal expansion and elastic properties are anisotropic. YAG on the other hand is cubic so its thermal expansion tensor is fully isotropic. As shown in Table 1, the Zener ratio of YAG is 1·04, so it is also nearly elastically isotropic as well.

Residual stress measurements were made on a YAG–Al_2O_3 DSE crystal approximately 2 mm in diameter that was grown by the laser-heated floating zone (LHFZ) method.[28] The orientation relationships found in these crystals were consistent with those previously published in the literature,[29] although the growth direction was different. Whereas only one orientation of YAG was found in the sample, two twin-related variants of Al_2O_3 were found. The variants, using rhomohedral indices for Al_2O_3, were:

$$[\bar{1}\bar{1}1]_{YAG}//[\bar{1}2\bar{1}]_{Al_2O_3}//\text{growth direction}$$

and

$$(2\bar{1}\bar{1})_{YAG}//(111)_{Al_2O_3} \text{ or } (2\bar{1}\bar{1})_{YAG}//(\bar{1}\bar{1}\bar{1})_{Al_2O_3}$$

The resulting stress tensors for the two phases are presented below with the reference frame outlined in Fig. 2 above:

YAG:

$$\begin{bmatrix} 43 & -26 & -71 \\ -26 & 18 & -111 \\ -71 & -111 & 119 \end{bmatrix} \pm \begin{bmatrix} 89 & 36 & 32 \\ 36 & 78 & 40 \\ 36 & 40 & 58 \end{bmatrix} \text{MPa}$$

Al_2O_3:

$$\begin{bmatrix} 16 & -72 & 21 \\ -72 & 3 & -18 \\ 21 & -18 & 67 \end{bmatrix} \pm \begin{bmatrix} 137 & 34 & 54 \\ 34 & 136 & 33 \\ 54 & 33 & 118 \end{bmatrix} \text{MPa}$$

Here x_3 is normal to the sample (parallel to the growth axis). The measured residual stresses in YAG-Al_2O_3 are up to two orders of magnitude less than those observed in NiO–ZrO_2, and most are approaching the magnitude of the experimental error.

5 Discussion

Residual stresses in directionally solidified ceramic eutectics arise from the thermal expansion mismatches between the two constituent phases. As seen in the example of NiO–cubic ZrO_2 DSEs, large residual stresses accumulate as the sample cools from the solidification temperature (in excess of 1700°C) to room temperature. The magnitudes of the stresses, on the order of one GPa tensile in NiO and compressive in ZrO_2, indicate that no significant plastic deformation processes transpired to mitigate the stresses. The ability of the composite to withstand these very high stresses without interfacial debonding, microfracturing or creep indicates that the two phases are strongly bonded at the interfaces even at high temperatures. The good interfacial adhesion is consistent with the idea that the interfaces are in a thermodynamically low-energy configuration. As seen in the case of NiO–cubic ZrO_2, the orientation relationship of the two crystals leads to a layered structure of anions and cation parallel to the interface with the two phases sharing a common oxygen plane at the interface (see Pennycook *et al.* in this issue).[22] It is interesting to note that other oxide heterophase systems maintain similar orientation relationships resulting in homopolar surfaces at the interface; these include NiO–CaO,[12] NiO–Y_2O_3,[11] Al_2O_3–ZrO_2(cubic)[30] and Fe_2O_3–Al_2O_3.[31] From the results of NiO–ZrO_2, it is inferred that these other systems may also share a common oxygen plane at the interface which leads to electrostatic bonding across the boundary. The fact that DSEs tend to form strongly bonded interfaces has significant consequences for the residual stress state of the materials since the interfaces are not prone to fracture or slip.

For a given DSE system, it is difficult to regulate the residual stress state, since neither the volume fractions nor the crystallographic orientation relationships can be controlled appreciably. Because there are few degrees of freedom, if low residual stresses are important, it is necessary to choose eutectics in which the two phases have similar thermal expansion behaviors. Such is the case for YAG–Al_2O_3 in which the thermal expansion properties are within approximately 5% of each other. Residual stress measurements by X-ray diffraction, presented above, indicate that no significant stresses are present at room temperature within the experimental measurement error. Upper estimates of predicted residual stresses for YAG–Al_2O_3 assuming complete interfacial constraint and a simplified lamellar geometry are on the order of 50 MPa, well below the measurement error. The large error associated with the YAG–Al_2O_3 residual stress measurements, on the order of 100 MPa, are attributed to gradients in the residual stresses across the sample. Since the diffraction technique used in these experiments measures average residual strains, such strain gradients increase the experimental uncertainty. Measuring residual stresses of the order of 100 MPa in ceramic materials is difficult by standard powder diffraction techniques since the corresponding elastic strains are very small, on the order of 10^{-2} percent strain.

The data for both the NiO–cubic ZrO_2 and YAG–Al_2O_3 are presented together in Fig. 5 for

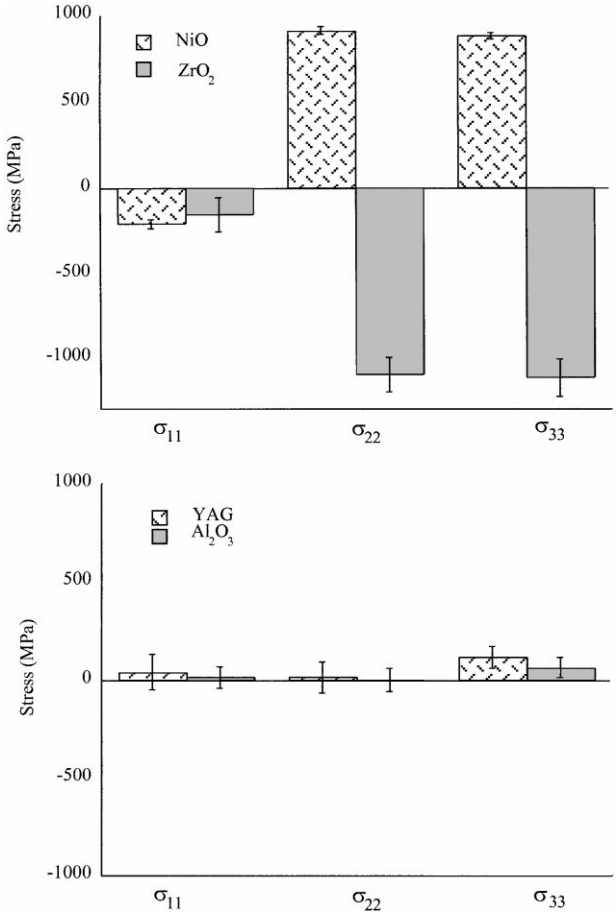

Fig. 5. Cumulative stress results for NiO–cubic ZrO_2 and YAG–Al_2O_3 presented together for visual comparison.

comparison. This figure highlights the effects of thermal expansion mismatches on the residual stress state of ceramic eutectic composites.

6 Conclusions

1. Residual stresses are of extreme concern in high-temperature ceramic composites, such as directionally solidified oxide eutectics, because the stresses ultimately affect the mechanical properties of the material. Ceramic materials are especially prone to thermal residual stresses because the processing temperatures are usually in excess of 1700°C.
2. Because directionally solidified eutectics are anisotropic and because the magnitude of the interfacial constraint between the two phases is not known *a priori*, it is desirable to measure the stresses experimentally.
3. Single crystal X-ray diffraction techniques can be used to measure the residual stress tensors of directionally solidified eutectic composites.
4. Systems in which there is a significant mismatch between the thermal expansion behaviors of the two phases, as in NiO–cubic ZrO_2, result in very large residual stresses at room temperature. The magnitude of the stresses, on the order of one GPa, indicate that the interfaces are very well bonded and that no significant plastic deformation occurs to mitigate the stresses.
5. YAG–Al_2O_3 is an example of a eutectic composite in which the two phases have very similar thermal expansion behaviors. Within the measurement accuracy, X-ray diffraction indicates that there are no appreciable residual stresses in these composites at room temperature.

Acknowledgements

The authors would like to thank Professor Alex Revcolevschi of the University de Paris-Sud and Dr Ali Sayir of NASA-Lewis Research Center for growing the eutectic crystals. This research was supported by the Southeastern Universities Research Association (SURA)/ORNL Summer Research Cooperative Program and the Assistant Secretary for Energy Efficiency and Renewable Energy, Office of Transportation Technologies as part of the High Temperature Materials Laboratory User Program at ORNL managed by Lockheed Martin Energy Research Corp. for the US Department of Energy under contract number DE-AC05-96OR22464.

References

1. He, M. Y. and Evans, A. G., Crack deflection at an interface between dissimilar elastic materials: role of residual stresses. *International Journal of Solids and Structures*, 1994, **31**, 3443–3455.
2. Kinloch, A. L., Thrusabanjong, E. and Williams, L. G., Fracture at bimaterial interfaces: the role of residual stresses. *Journal of Materials Science*, 1991, **26**, 6260–6270.
3. Nye, L. F., *Physical Properties of Crystals*. Oxford Science Publications, Oxford, 1985.
4. Hulse, C. O. and Batt, J. A. The effect of eutectic microstructure on the mechanical properties of ceramic oxides. United Aircraft Research Laboratories, report #N910803-10, 1974.
5. Ashbrook, R. L., Directionally solidified ceramic eutectics. *Journal of the American Ceramic Society*, 1977, **60**, 428–435.
6. Mah, T., Parthasarathy, T. A. and Matson, L. E., Processing and mechanical properties of $Al_2O_3/Y_3Al_5O_{12}$ (YAG) eutectic composite. *Ceramic Engineering and Science Proceedings*, 1990, **11**, 1617–1627.
7. Parthasarathy, T. A. and Mah, T., Creep behavior of an $A1_2O_3$–$Y_3Al_5O_{12}$ eutectic composite. *Ceramic Engineering and Science Proceedings*, 1990, **11**, 1628–1638.
8. Cooksey, D. J. S., Munson, D., Willkinson, M. P. and Hellawell, A., *Philosophical Magazine*, 1964, **10**, 745.
9. Stubican, V. S. and Bradt, R. C., Eutectic solidification in ceramic systems. *Annual Reviews in Materials Science*, 1981, **11**, 267–297.
10. Minford, W. J., Brandt, R. C. and Stubican, V. S., Crystallography and microstructure of directionally solidified oxide eutectics. *Journal of the American Ceramic Society*, 1979, **62**, 154–157.
11. Fragneau, M., Revcolevschi, A. and Michel, D., Crystallography of directionally solidified NiO–Y_2O_3 eutectic.

Journal of the American Ceramic Society, 1982, **65**, C102–103.
12. Fragneau, M. and Revcolevschi, A., Crystallography of the directionally solidified NiO–CaO eutectic. *Journal of the American Ceramic Society*, 1983, **66**, C162–C163.
13. Noyan, I. C. and Cohen, J. B., Residual stress, measurement by diffraction and interpretation. In *Materials Research and Engineering*, ed. B. Ilschner and N. J. Grant. Springer–Verlag, New York, 1986, p. 276.
14. Reimers, W., Investigation of large grained samples-principles. In *Measurement of Residual and Applied Stresses Using Neutron Diffraction*, ed. M. T. Hutchings and A. D. Krawitz. Kluwer Academic Publishers, Dordrecht/Boston/London, 1992, pp. 159–170.
15. Reimers, W., Crostack, H.-A., Wrobel, M. and Eckold, G., Investigations of large grained samples—examples. In *Measurement of Residual and Applied Stresses Using Neutron Diffraction*, ed. M. T. Hutchings and A. D. Krawitz. Kluwer Academic Publishers, Dordrecht/Boston/London, 1992, pp. 263–273.
16. Derraz, Y., Lavelle, B. and Durand, L. X-ray determination of the microstress tensor of a twinned grain in polycrystalline nickel. In *Proceedings of the Fourth International Conference on Residual Stresses, Baltimore, MD 1994*, pp. 312–116.
17. Dupke, R. and Reimers, W., X-ray diffraction investigations on individual grains in the polycrystalline Ni-base superalloy in 939 during cyclical loading II: residual stresses. *Zeitschrift Fur Metalikunde*, 1995, **86**, 665–670.
18. Dickey, E. C., Hubbard, C. R. and Dravid, V. P., Interlamellar residual stresses in single grains of a NiO–ZrO_2(cubic) directionally solidified eutectic. *Journal of the American Ceramic Society*, 1997, **80**, 2773–2780.
19. Clemens, B. M. and Bain, L. A. Stress determination in textured thin films using X-ray diffraction. *MRS Bulletin*, 1992, July, 46–51.
20. Press, W. H., Teukolsky, S. A., Vetterling, W. T. and Flannery, B. P., *Numerical Recipies in Fortran*, 2nd edn. Cambridge University Press, Cambridge, 1992 p. 963.
21. Dhalenne, G. and Revcolevschi, A., Directional solidification in the NiO–ZrO_2 system. *Journal of Crystal Growth*, 1984, **69**, 616–618.
22. Dickey, E. C., Dravid, V. P., Nellist, P. D., Wallis, D. J. and Pennycook, S. J., Three-dimensional atomic structure of NiO–ZrO_2(cubic) interfaces. *Acta Materialia*, 1998, **46**, 1801–1816.
23. Touloukian, Y. S., *Thermophysical Properties of High Temperature Solid Materials, vol. 4, Oxides and their Solutions and Mixtures*. MacMillan, New York, 1967.
24. Gupta, T. K. and Valentich, J., *Journal of the American Ceramic Society*, 1971, **54**, 355–356.
25. Uchida, N., Saito, S. Elastic constants and acoustic absorption coefficients in MnO, CoO, and NiO single crystals at room temperature. *The Journal of the Acoustical Society of America*, 1971, **51**, 1602–1605.
26. Ingel, R. P. and Lewis III, D., Elastic anisotropy in zirconia single crystals. *Journal of the American Ceramic Society*, 1988, **71**, 265–271.
27. Hellwege, K.-H. and Hellwege, A. M. (eds), *Numerical Data and Functional Relationships in Science and Technology*. New Series Vol. 11, K. H. Hellwege, Springer–Verlag Berlin, 1979.
28. Sayir, A. and Matson, L. E., Growth and characterization of directionally solidified $Al_2O_3/Y_3Al_5O_{12}$ (YAG) eutectic fibers. In *Proceedings of the 4th Annual HITEMP Review*. NASA Conference Publication, Cleveland, OH, 1991, 83.1–83.13
29. Hay, R. S. and Matson, L. E., Aluniina/yttrium-alunminum gamet crystallographic orientation relationships and interphase boundaries: observations and interpretation by geometric criteria. *Acta Metallurgica and Materialia*, 1991, **39**, 1981–1994.
30. Mazerolles, L., Michel, D. Cornier, M. and Portier, R., Interfaces between zirconia and refractory oxides. In *Advances in Ceramics Science and Technology of Zirconia III*. The American Ceramic Society, 1988.
31. Tietz, L. A. and Carter, C. B., Structure of the Fe_2O_3–Al_2O_3 (1102) interface. *Philosophical Magazine A*, 1993, **67**, 729–744.